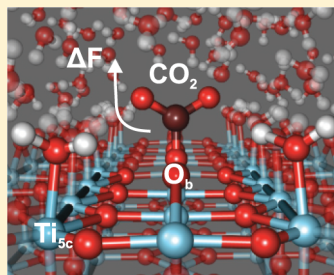


CO₂ Adsorption and Reactivity on Rutile TiO₂(110) in Water: An *Ab Initio* Molecular Dynamics Study

Konstantin Klyukin[†] and Vitaly Alexandrov^{*,†,‡}[†]Department of Chemical and Biomolecular Engineering and [‡]Nebraska Center for Materials and Nanoscience, University of Nebraska–Lincoln, Lincoln, Nebraska 68588, United States

Supporting Information

ABSTRACT: Atomic-scale understanding of CO₂ adsorption and reactivity on TiO₂ is important for the development of new catalysts for CO₂ conversion with improved efficiency and selectivity. Here, we employ Car–Parrinello molecular dynamics combined with metadynamics simulations to explore the interaction dynamics of CO₂ and rutile TiO₂(110) surface explicitly treating water solution at 300 K. We focus on understanding the competitive adsorption of CO₂ and H₂O, as well as the kinetics of CO and bicarbonate (HCO₃[−]) formation. Our results show that adsorption configurations and possible reaction pathways are greatly affected by proper description of the water environment. We find that in aqueous solution, CO₂ preferentially adsorbs at the bridging oxygen atom O_b, while Ti_{5c} sites are saturated by H₂O molecules that are difficult to displace. Our calculations predict that further conversion reactions include spontaneous protonation of adsorbed CO₂ and detachment of OH[−] to form a CO molecule that is significantly facilitated in the presence of a surface Ti³⁺ polaron. In addition, the mechanisms of HCO₃[−] formation in bulk water and near TiO₂(110) surface are discussed. These results provide atomistic details on the mechanism and kinetics of CO₂ interaction with TiO₂(110) in a water environment.



INTRODUCTION

The problem of anthropogenic CO₂ emissions has been recently attracting a lot of attention due to a dramatic rise of CO₂ in the atmosphere in the past few decades.^{1–3} One efficient way to counterbalance CO₂ emissions is to photocatalytically convert CO₂ to valuable chemicals such as methanol (CH₃OH), methane (CH₄), formic acid (HCOOH), and formaldehyde (H₂CO) using renewable solar energy.^{2–6} Among various photocatalysts, anatase and rutile phases of titanium dioxide (TiO₂) have been extensively examined both experimentally and theoretically. Despite a great deal of prior research,^{5,7–15} both the efficiency and selectivity of CO₂ conversion reactions over TiO₂ catalysts are still poor, and the reaction mechanisms are not yet well understood at the atomic level.

Many catalytic CO₂ conversion reactions are experimentally carried out in aqueous solution, while previous theoretical investigations have been limited to consideration of CO₂ reaction mechanisms in the gas phase^{7–10} and primarily for the anatase polymorph of TiO₂.^{13,16–18} It is well established, however, that the presence of a solvent can play a critical role in determining both the rates and pathways of various reactions including CO₂ conversion. For example, it is known that methanol is the major product in the gas-phase reduction of CO₂ on Cu catalysts, whereas methane is the predominant species in the aqueous electrocatalytic reduction process.^{19,20}

Some recent first-principles computational studies^{7,9} have indeed demonstrated that the presence of even one H₂O molecule coadsorbing with CO₂ on different TiO₂ surfaces can change the binding energy of CO₂ by as much as 0.25 eV

relative to the case with no water.⁷ Moreover, not only can the stability of CO₂ molecule on the TiO₂ surfaces be modified by water environment, but also the stability and reactivity of reaction intermediates. Although some of the previous theoretical works have explored the effect of H₂O molecule coadsorption on the reaction mechanisms of surface-mediated CO₂ conversion, most of the studies have been limited to introducing the aqueous environment through the implicit solvent model. This model, however, cannot account for the formation and dynamics of hydrogen bonding network that greatly affect CO₂ adsorption and surface-mediated reaction mechanisms.¹⁹

In recent years, computational techniques such as metadynamics that allow one to avoid the limitations of traditional *ab initio* molecular dynamics (AIMD) to sample the free energy landscape have been gaining much attention.^{9,16,19,21} Recently, AIMD-based metadynamics simulations were successfully employed to unveil the mechanisms and kinetics of various interfacial reactions including electrochemical reduction of CO₂ and CO in aqueous solutions at room temperature over model catalyst surfaces such as the Cu(100) facet.^{19,22,23}

COMPUTATIONAL METHODOLOGY

In this study, we carry out density-functional-theory (DFT) Car–Parrinello molecular dynamics (CPMD) simulations to allow explicit treatment of water and temperature effects on

Received: March 23, 2017

Revised: April 24, 2017

Published: April 25, 2017

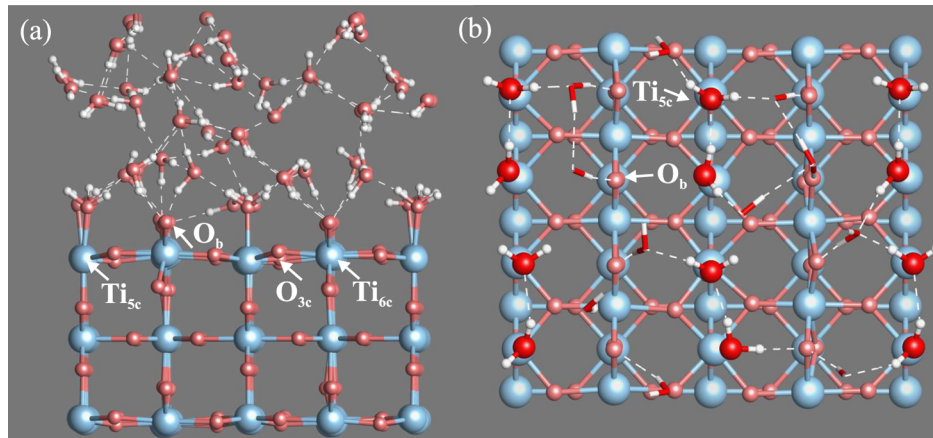


Figure 1. Side (a) and top (b) views of the interfacial water structure at the rutile $\text{TiO}_2(110)$ surface from CPMD simulations. Color code: Ti, blue; O, red; H, white. The water molecules of the first layer are represented by a ball and stick model, the dashed lines highlight the hydrogen bonds network.

CO_2 adsorption and reactivity at the rutile $\text{TiO}_2(110)$ surface. To obtain free-energy reaction barriers, we utilize a CPMD-based metadynamics technique that allows accelerated sampling of reaction pathways characterized by a set of collective variables (CVs), as implemented in the NWChem software package.²⁴ Previously, metadynamics simulations have been successfully applied to examine the mechanisms and rates of a variety of rare-event chemical reactions,^{9,16,19,21} and the theoretical background of this approach was described in detail elsewhere.^{25,26} Full details of our computational protocol can be found in the Supporting Information, while here we just briefly describe the key features of the computational scheme.

The rutile $\text{TiO}_2(110)$ surface was modeled as a periodic slab comprised of the three TiO_2 layers (the central layer was fixed) with a 4×2 surface supercell and a vacuum gap of 10 \AA , thus resulting in a $13.38 \times 11.91 \times 19.98 \text{ \AA}^3$ simulation cell. To provide a water density of about 1 g/cm^3 , the vacuum gap was filled with one CO_2 and 55 H_2O molecules (see Figure 1). All calculations were performed at the Γ point using the Perdew–Burke–Ernzerhof (PBE) exchange-correlation functional,²⁷ Troullier–Martins²⁸ pseudopotentials for Ti, and Hamann-type²⁹ pseudopotentials for H, C, and O atoms. The kinetic energy cutoff of 60 Ry was employed, while a larger energy cutoff of 100 Ry was found to yield very similar CO_2 desorption energetics (0.65 eV for the adsorption position O_b-CO_2 , as compared with 0.67 eV at 60 Ry). The PBE functional was corrected for long-range dispersion interactions using the Grimme approach (DFT-D4).³⁰ The temperature of the simulation cell was maintained constant at 300 K employing a Nose–Hoover thermostat.^{31,32} To achieve thermal stability, 6 ps quantum mechanics/molecular mechanics (QM/MM) simulations were first carried out to pre-equilibrate the water/ $\text{TiO}_2(110)$ interface followed by 6 ps of CPMD equilibration. Then each adsorption configuration was additionally equilibrated for ~ 5 ps to provide energy conservation within 10^{-3} eV/ps. For each adsorbed state, we used several slightly different starting configurations. The equilibration procedure used in this study is similar to some previous AIMD studies of water/metal oxide interfaces including TiO_2 .^{16,19,21,33} The CPMD production trajectories were 6 ps long, while metadynamics simulations were run for 4–12 ps depending on the system. For the reactions involving a surface Ti^{3+} polaron, we employ the GGA+U formalism³⁴ with $U_{\text{eff}} = 5$

eV based on previous theoretical studies of polarons in TiO_2 .^{35,36}

RESULTS AND DISCUSSION

TiO₂(110)/Water Interface. We start by considering the structure of interfacial water and energetics of water desorption from the hydroxylated $\text{TiO}_2(110)$ surface, which is important due to the competition between H_2O and CO_2 molecules in the aqueous phase for surface adsorption. The molecular structure of water– $\text{TiO}_2(110)$ interface was previously examined in a number of experimental^{37–40} and first-principles computational^{37,40–44} investigations, and our CPMD results reported here are in full agreement with a recent detailed study by *in situ* scanning probe microscopy.⁴⁰ The rutile $\text{TiO}_2(110)$ surface layer contains the 5- and 6-fold coordinated Ti atoms (Ti_{5c} and Ti_{6c} , respectively), 3-fold coordinated O atoms (O_{3c}) and 2-fold coordinated bridging O atoms (O_b), as depicted in Figure 1. As an initial state for all calculations the uppermost surface of the slab was saturated by H_2O molecules attached to the undercoordinated surface Ti_{5c} cations, while the rest of the vacuum gap was filled randomly with H_2O molecules before starting QM/MM followed by CPMD simulations.

We did not observe any water dissociation over the TiO_2 surface during equilibration at 300 K, in accordance with previous first-principles modeling studies.^{42,43} For the equilibrated state, we find that the first interfacial layer of water along the Ti_{5c} rows exhibits molecular ordering characterized by a water–dimer structural motif as shown in Figure 1, in full agreement with a recent first-principles molecular dynamics investigation.⁴⁰ Such interfacial structure is different from a one-dimensional chain structure along the Ti_{5c} rows suggested by static DFT calculations⁴⁴ and is due to the interaction between H_2O molecules of the first and second water layers through the hydrogen bonding network. Specifically, we identify a stable network of hydrogen bonds between O_b atoms, adsorbed H_2O at the Ti_{5c} sites, and the H_2O molecules in the second hydration layer. The third and farther water layers do not interact directly with the TiO_2 surface and can be considered as the bulk liquid phase.

To analyze the energetics of the H_2O desorption process, we only consider desorption of H_2O from the Ti_{5c} site, since H_2O molecules interacting with other surface sites through the hydrogen bonds are expected to be labile at 300 K. Figure 2

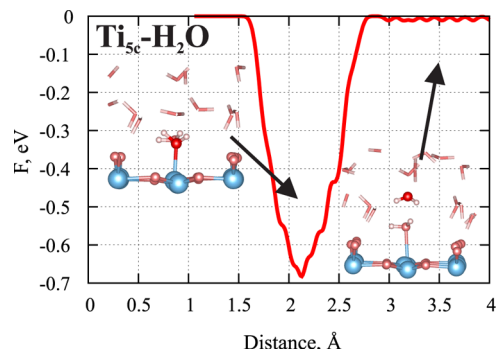


Figure 2. Free-energy profile of H_2O desorption reaction from the Ti_{5c} surface site as computed using CPMD metadynamics simulations with the distance (in Å) between adsorbed H_2O and $\text{TiO}_2(110)$ surface used as a collective variable. The initial and final states are shown on the left and right, respectively.

shows the free-energy profile of the desorption reaction based on CPMD metadynamics simulations as a function of the bond distance between Ti_{5c} and O_w of the H_2O molecule leaving the surface. It is seen that when the bond distance becomes larger than 3 Å, the desorption reaction can be considered complete. The activation barrier for H_2O desorption is estimated at 0.69 eV, thus being in the experimental range of 0.6–1.05 eV,^{10,45} but it is smaller than the values of 0.77 eV⁴² and 0.99 eV⁹ estimated previously from DFT with no explicit treatment of water at 0 K. Our smaller value can be explained by additional stabilization of the desorbed H_2O molecule due to the hydrogen bonding network of the bulk water.

CO₂ Adsorption and Reduction. We next examine different CO_2 adsorption configurations at the $\text{TiO}_2(110)$ surface in the presence of water at 300 K. Out of six adsorption states observed in previous static DFT calculations at 0 K,^{7,9} only two are found to be stable after a few picoseconds of CPMD simulations, as shown in Figure 3. The first stable adsorption state is $\text{O}_b\text{-CO}_2$ (Figure 3b), where CO_2 is adsorbed at the bridging oxygen atom O_b . The average $\text{O}_b\text{-C}$ bond distance during 5 ps trajectory is 1.365 Å, while the O–C–O angle is about 124.7°. This is very close to that of the CO_2^- molecule in the gas phase (138°)⁴⁶ and much smaller than that found for the adsorbed CO_2 in DFT-PBE calculations with no water at 0 K (178°).^{7,9} This suggests that some activation has occurred owing to the electron transfer from the TiO_2 surface to the adsorbed CO_2 species. A number of other configurations such as CO_2 at the O_b site rotated by 90° around the z axis relative to the $\text{O}_b\text{-CO}_2$ configuration (Figure 3a) and CO_2 located between two adjacent bridging O_b atoms (Figure 3c) switched to the $\text{O}_b\text{-CO}_2$ configuration after a few picoseconds.

It is believed that electron transfer from the TiO_2 surface to adsorbed CO_2 activates the molecule toward further reactions via the formation of a bent CO_2^- species.^{7,47} It was estimated in static DFT calculations that a relatively low energy barrier of 0.27 eV is required to activate a planar physisorbed CO_2 molecule to a bent adsorbed configuration.⁹ In our calculations, we observe that the physisorbed CO_2 molecule is weakly bound to the $\text{TiO}_2(110)$ surface and may spontaneously leave the surface during CPMD. We also see (Figure 1b) that the second layer of water bounded to O_b may also hinder CO_2 physisorption. Thus, despite the predicted low barrier, CO_2 adsorption and further activation appears to be the rate-limiting step of CO_2 reduction.^{6,48} It was also hypothesized that

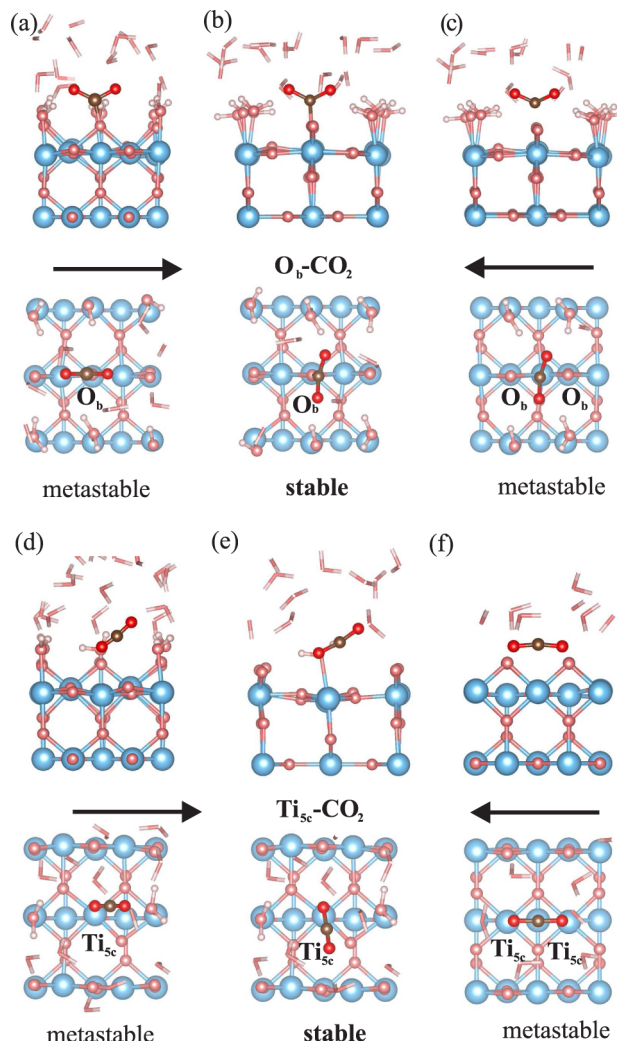


Figure 3. Side and top views of the main adsorption configurations of CO_2 on the rutile $\text{TiO}_2(110)$ surface. (a–c) CO_2 adsorbed on a bridge oxygen (O_b); (d–f) CO_2 adsorbed on the five-coordinated Ti atom (Ti_{5c}).

photogeneration of an electron–hole pair might contribute to this activation; however, the role of this process in CO_2 activation is still unclear, and a DFT study of excited stoichiometric anatase TiO_2 surface has shown no tendency for electron transfer from the surface to adsorbed CO_2 .⁴⁹ Thus, our results suggest that CO_2 in aqueous solution is partially activated in the $\text{O}_b\text{-CO}_2$ configuration; however, the presence of an electron–hole pair or intrinsic surface defects can additionally contribute to CO_2 activation.

The second stable adsorption state is $\text{Ti}_{5c}\text{-CO}_2$, which is a monodentate adsorbed CO_2 molecule bound to the Ti_{5c} site via an oxygen of CO_2 in a tilted configuration (Figure 3e). The average bond distance $\text{Ti}-\text{O}$ is equal to 2.674 Å, and the O–C–O angle is 173.2°. A similar 90° rotated configuration (Figure 3d) is found to be metastable and switched to $\text{Ti}_{5c}\text{-CO}_2$. The bidentate configuration of CO_2 adsorbed along the Ti_{5c} row (Figure 3f) is also found to be metastable and changed to the $\text{Ti}_{5c}\text{-CO}_2$ adsorption state.

The adsorption energies of CO_2 on TiO_2 surfaces are known to be greatly affected by introducing a water environment. Specifically, the binding energy of CO_2 was determined to be larger by ~0.1–0.2 eV when considering coadsorption with a

single H_2O ^{7,9} and by ~ 0.3 eV when applying an implicit solvent model.⁷ A comparison of DFT calculated adsorption energies for CO_2 on TiO_2 in various models is provided in Table 1.

Table 1. Adsorption Energies (in eV) of a Single CO_2 Molecule at the O_{b} and Ti_{sc} Surface Sites with None (E_{ads}) and Two Coadsorbing H_2O Molecules (E_{coads}), As Well As Employing Implicit Solvent Model (E_{ISM}) Based on Zero-Temperature DFT Calculations^a

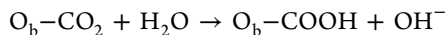
	E_{ads}	E_{coads}	E_{ISM}
$\text{O}_{\text{b}}-\text{CO}_2$	0.22, ⁷ 0.29 ⁹	0.63, 0.46, ⁷ 0.54 ⁹	0.83 ⁷
$\text{Ti}_{\text{sc}}-\text{CO}_2$	0.33, ⁷ 0.46 ⁹	0.41, 0.42, ⁷ 0.49 ⁹	0.75–0.81 ⁷

^a Adsorption energy of a single H_2O molecule at Ti_{sc} estimated as 1.01 eV is provided for comparison.

Overall, the results suggest that CO_2 is thermodynamically equally stable at the Ti_{sc} and O_{b} surface sites, whereas H_2O is stronger adsorbed to the rutile surface (at the Ti_{sc} site) than CO_2 (at any site). Thus, CO_2 molecules are expected to preferentially bind to the O_{b} sites based on zero-temperature DFT results. To better understand the competitive adsorption/desorption between H_2O and CO_2 at the rutile surface in water at 300 K, we perform additional free-energy calculations to estimate CO_2 desorption barriers and compare it with the H_2O case.

Figure 4 shows the simulated free-energy profiles of CO_2 desorption from Ti_{sc} and O_{b} surface sites, while Table 2 summarizes the estimated desorption barriers for all species considered in this study. It is apparent that not only H_2O has a higher adsorption energy than CO_2 (Table 1), but also it is much more difficult to desorb it from the Ti_{sc} site (Table 2). On the other hand, it is considerably more energetically difficult to displace adsorbed CO_2 from the O_{b} site than from Ti_{sc} site. Therefore, our results suggest that in aqueous environment the Ti_{sc} sites should be filled with H_2O molecules, while CO_2 preferentially adsorbs on the O_{b} sites.

For the most stable $\text{O}_{\text{b}}-\text{CO}_2$ configuration we observe spontaneous protonation of the adsorbed CO_2 molecule during CPMD with a proton coming from the H_2O molecule adsorbed at the neighboring Ti_{sc} site according to the following reaction:



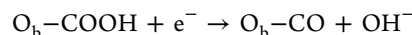
The driving force for such a spontaneous proton shuttling can be the activated character of ${}^*\text{COO}$ (${}^*\text{COO}$ denotes adsorbed COO) in this configuration. Figure 5 illustrates how the adsorbed CO_2 molecule exchanges an H atom with the

Table 2. Comparison of Free-Energy Barriers (in eV) of CO_2 , H_2O , and HCO_3^- Desorption from the O_{b} and Ti_{sc} Sites of the Rutile $\text{TiO}_2(110)$ Surface in Aqueous Solution from CPMD-Based Metadynamics Simulations

$\text{O}_{\text{b}}-\text{CO}_2$	$\text{Ti}_{\text{sc}}-\text{CO}_2$	$\text{Ti}_{\text{sc}}-\text{H}_2\text{O}$	$\text{Ti}_{\text{sc}}-\text{HCO}_3^-$ (monodentate)	$\text{Ti}_{\text{sc}}-\text{HCO}_3^-$ (bidentate)
0.67	0.27	0.69	0.49	0.87

neighboring H_2O molecules during 6.5 ps CPMD time frame. As seen from Figure 5 at any instance of time, only one (or none) of the two nearest-neighbor H atoms can be bound to the CO_2 molecule: when the first proton becomes bound, the second is repelled from CO_2 . When considering CO_2 desorption, however, CO_2 always leaves the surface with no protons attached. Thus, our simulations demonstrate that there is a dynamic equilibrium between adsorbed ${}^*\text{COO}$ and ${}^*\text{COOH}$ species at the O_{b} surface site.

We next analyze the reduction of CO_2 to CO , which was experimentally shown to be the dominant reaction pathway on pure $\text{TiO}_2(110)$ surface.⁴⁷ According to a previously proposed mechanism,^{4,5,50} we consider the following reaction of CO formation through dehydroxylation of ${}^*\text{COOH}$ formed at the surface:



It was previously demonstrated in static DFT calculations that the surface Ti^{3+} polaron is more stable at Ti_{sc} than at Ti_{sc} site.^{35,36} Moreover, we find that Ti^{3+} polaron is indeed stable at Ti_{sc} during metadynamics simulations at 300 K, with an electron eventually being transferred to the ${}^*\text{COOH}$ molecule followed by dehydroxylation reaction. On the contrary, an attempt to stabilize the polaron at Ti_{sc} was not successful, and after a short period of time we observe spontaneous protonation of the surface O_{b} atom by a nearby H_2O molecule accompanied by electron delocalization from the Ti_{sc} site.

Figure 6 compares the free-energy profiles of CO formation from ${}^*\text{COOH}$ obtained with and without surface Ti^{3+} polaron. Our calculations indicate that the presence of Ti^{3+} polaron facilitates the dehydroxylation of COOH substantially by making the energy barrier of the reaction almost twice lower than without a polaron. This result is completely consistent with experimental observations of the absence of this reaction in the dark⁵¹ and significant reaction acceleration on oxygen-deficient surfaces,⁴⁸ where the oxygen vacancies provide excess electrons to the rutile $\text{TiO}_2(110)$.

Formation of HCO_3^- Species and Their Stability. The formation of bicarbonate HCO_3^- species was detected in a

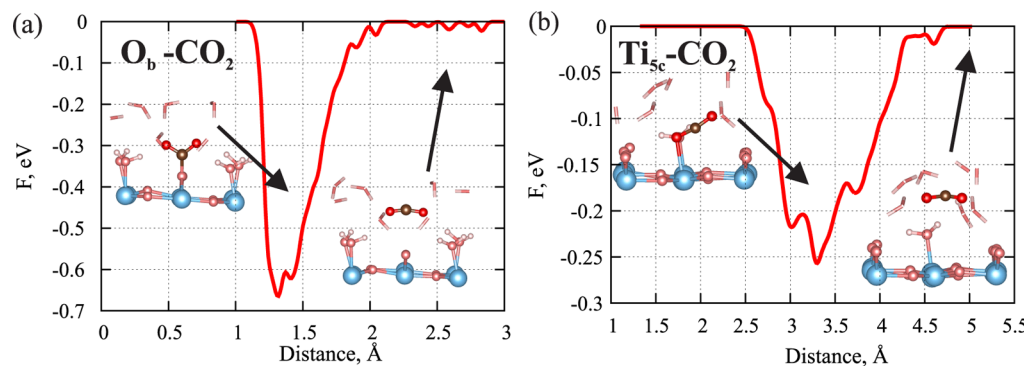


Figure 4. Free-energy profiles of CO_2 desorption reaction from (a) O_{b} site and (b) Ti_{sc} site of the $\text{TiO}_2(110)$ surface.

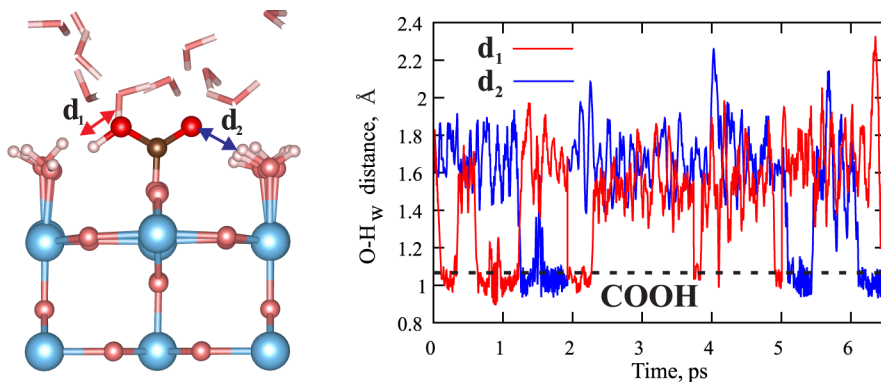


Figure 5. Illustration of CO₂ protonation/deprotonation reaction during 6.5 ps CPMD run with proton shuttling between adsorbed CO₂ and nearby H₂O molecules. The O–H_w distance less than 1.05 Å means that an H belongs to the CO₂ molecule.

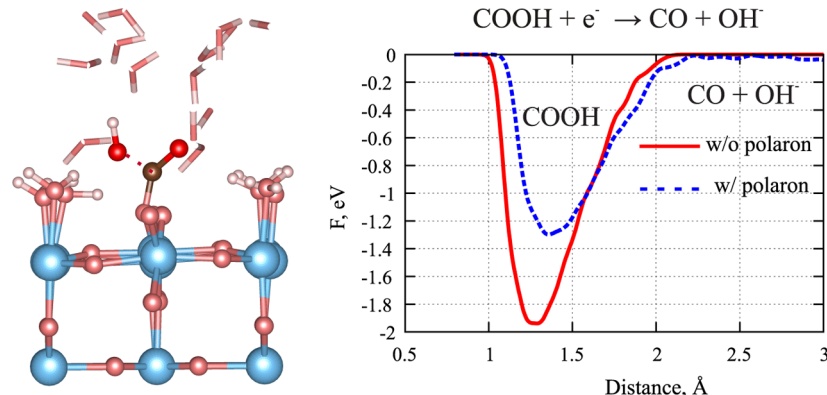


Figure 6. Free-energy profiles of CO formation from the adsorbed COOH molecule with and without a surface Ti³⁺ polaron as computed by CPMD metadynamics within the GGA+U approach.

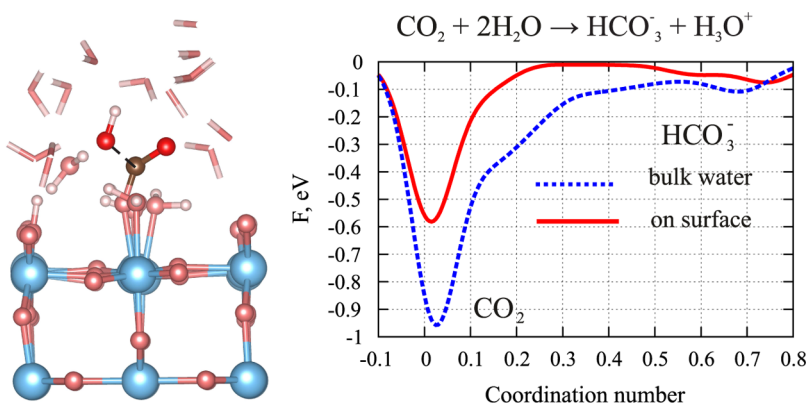
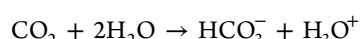


Figure 7. Free-energy profiles along the reaction pathway of HCO₃⁻ formation near the TiO₂(110) surface and in the bulk water. The energy profile is computed using the coordination number of a C atom with O atoms from water as a collective variable. The energy profile is plotted against Coordination number. The value of ~0.7 means that C is bound to OH, forming HCO₃⁻.

number of experiments,^{15,52} while HCO₃⁻ was not observed in some other experiments at the surface under ambient conditions.⁵² It was also found that under supercritical conditions, almost all CO₂ in water solution can be transformed to HCO₃⁻.⁵³ HCO₃⁻ formation is assumed to play an important role in the CO₂ conversion process in aqueous solution since the monolayer of bicarbonate can block the catalyst surface. Therefore, to gain insight into the mechanism of HCO₃⁻ formation reaction both in the bulk water and at the TiO₂(110) surface, we analyze HCO₃⁻ stability on different

surface sites and the competition for these sites between HCO₃⁻ and H₂O adsorption/desorption.

The formation of HCO₃⁻ species can proceed according to the following reaction:



In order to evaluate the catalytic effect of the TiO₂(110) surface in bicarbonate formation, we compare the kinetics of this reaction in bulk water and at the rutile surface based on metadynamics simulations. In the bulk water case, the reaction was simulated in a periodic cubic box of length 13 Å filled with

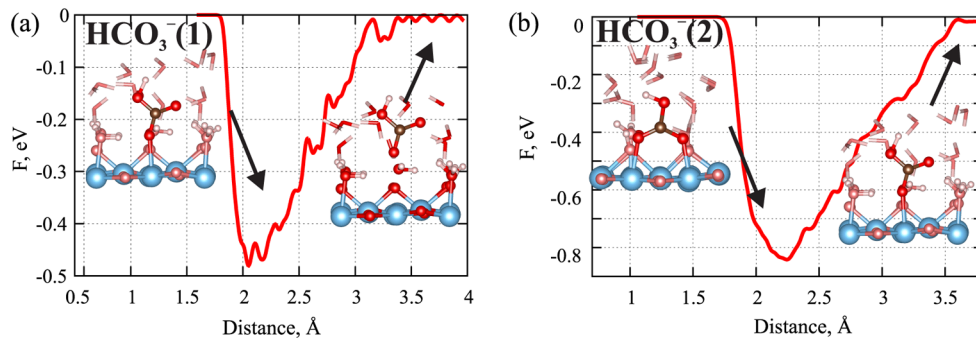


Figure 8. Main adsorption configurations of HCO_3^- on the $\text{TiO}_2(110)$ surface and the corresponding free-energy profiles for desorption reactions.

74 H_2O molecules and one CO_2 molecule using the same CPMD computational protocol as before. To drive the reaction, the number of water oxygen atoms bound to the carbon atom was used as a collective variable. We observe that in the proximity of the barrier crossing, CO_2 becomes activated by bending toward a neighboring H_2O molecule, and after that the H_2O deprotonation occurs. The estimated free-energy barrier of the reaction in bulk water is about 0.85 eV (Figure 7), which is in excellent agreement with the experimental value (0.95 eV)⁵⁴ and previous CPMD calculations using a similar computational protocol (0.82 eV).²¹

For the most favorable adsorption configuration of CO_2 on TiO_2 (O_b-CO_2) we could not drive HCO_3^- formation in metadynamics simulations, partially due to the unfavorable steric effect of this CO_2 configuration. By contrast, the reaction at Ti_{Sc} proceeds with an activation barrier of 0.59 eV, which is significantly reduced with respect to the bulk water case (0.85 eV). Based on our results described above, however, we expect most of the Ti_{Sc} sites to be occupied by H_2O molecules that are difficult to displace. We also observe that H_3O^+ formed during this reaction immediately splits into an H_2O molecule and an H^+ ion which is then trapped by the nearby bridging oxygen O_b atom (see Figure 7). Thus, our calculations suggest that some of the surface O_b sites may be protonated as the result of HCO_3^- formation. At low pH the O_b sites are expected to be already protonated, diminishing the probability of bicarbonate formation from CO_2 adsorbed at Ti_{Sc} , whereas high pH should facilitate the reaction. Also, at high pH the formation of bicarbonate will be also facilitated due to CO_2 reaction with OH^- groups in solution, which is characterized by a much smaller free-energy barrier of 0.6 eV than between CO_2 and H_2O (0.82 eV).^{21,55}

Another reaction mechanism of HCO_3^- formation at the TiO_2 surface has been recently hypothesized in experiments on TiO_2 with bimetallic clusters.¹¹ This mechanism suggests the participation of TiO_2 lattice oxygen atoms in oxidation of the protonated CO_2 species at the surface. As discussed above, we indeed observe spontaneous protonation of CO_2 in the O_b-CO_2 configuration to yield ${}^*\text{COOH}$ and thus explore the kinetics of the reaction $\text{O}_b-\text{COOH} \rightarrow \text{HCO}_3^- (\text{aq})$. We find, however, that this reaction pathway is characterized by a very high activation barrier of ~ 2 eV.

In the following, we examine several plausible adsorption configurations of HCO_3^- on the $\text{TiO}_2(110)$ surface. Among different possibilities, we determine two configurations that stay stable after 5 ps CPMD run. The first stable state is a $\text{HCO}_3^-(1)$ molecule adsorbed in a monodentate way at Ti_{Sc} (Figure 8a). The average distance between surface Ti_{Sc} and O is found to be 2.201 Å and the free energy of desorption from this

configuration is estimated at 0.49 eV. Thus, HCO_3^- is predicted to be bound to the Ti_{Sc} site considerably stronger than CO_2 , but weaker than H_2O .

Figure 8 shows the second stable state of a $\text{HCO}_3^-(2)$ molecule, which is bidentate adsorbed at two adjacent Ti_{Sc} sites. The average O– Ti_{Sc} distance is now 2.163 Å, which is slightly shorter than the Ti–O distance for the monodentate adsorbed configuration. The desorption process of bidentate configuration $\text{HCO}_3^-(2)$ is considered in two steps: (a) breaking one of the two bonds and thereby switching the molecule to monodentate configuration $\text{HCO}_3^-(1)$ and then (b) detachment of a monodentate $\text{HCO}_3^-(1)$ molecule. The metadynamics simulation reveal that HCO_3^- is very strongly bound to two surface Ti_{Sc} atoms and the free energy to break the first bond is 0.87 eV. Thus, the obtained results prompt that the formation of a very tightly bound bicarbonate monolayer on the rutile (110) surface could block all of the unsaturated Ti atoms and prevents all the described above reactions of CO_2 reduction,¹⁵ but only if strongly bound H_2O molecules had been displaced from Ti_{Sc} .

CONCLUSIONS

In summary, Car–Parrinello molecular dynamics in conjunction with metadynamics simulations were used to describe the competitive adsorption/desorption behavior of CO_2 and H_2O over the rutile $\text{TiO}_2(110)$ surface in water environment at room temperature. It was determined that in the aqueous phase CO_2 preferentially adsorbs at the bridging oxygen (O_b) atoms, while Ti_{Sc} sites are saturated by strongly bound H_2O molecules. Our calculations reveal that CO_2 is spontaneously protonated in the adsorbed state leading to the formation of activated ${}^*\text{COOH}$ species at the surfaces, and the kinetics of OH^- detachment to form CO is greatly enhanced in the presence of a Ti^{3+} polaron. The calculations also suggest that if tightly bound H_2O molecules are displaced from Ti_{Sc} sites, then the $\text{TiO}_2(110)$ surface catalyzes the formation of surface-bound HCO_3^- species that will block the surface from further reactions.

ASSOCIATED CONTENT

S Supporting Information

The Supporting Information is available free of charge on the ACS Publications website at DOI: 10.1021/acs.jpcc.7b02777.

Detailed description of the atomistic model, Car–Parrinello molecular dynamics, and metadynamics simulations with all computational parameters (PDF)

AUTHOR INFORMATION

Corresponding Author

*E-mail: valexandrov2@unl.edu; Phone: +1 402 4725323.

ORCID

Konstantin Klyukin: [0000-0001-8325-8725](https://orcid.org/0000-0001-8325-8725)

Notes

The authors declare no competing financial interest.

ACKNOWLEDGMENTS

The Holland Computing Center at the University of Nebraska-Lincoln is acknowledged for computational support. This work used the Extreme Science and Engineering Discovery Environment (XSEDE)⁵⁶ computing resource, which is supported by the National Science Foundation. V.A. also gratefully acknowledges financial support from the startup package provided by the University of Nebraska-Lincoln.

REFERENCES

- (1) Arakawa, H.; Aresta, M.; Armor, J. N.; Barreau, M. A.; Beckman, E. J.; Bell, A. T.; Bercaw, J. E.; Creutz, C.; Dinjus, E.; Dixon, D. A.; et al. Catalysis research of relevance to carbon management: progress, challenges, and opportunities. *Chem. Rev.* **2001**, *101*, 953–996.
- (2) Centi, G.; Perathoner, S. Opportunities and prospects in the chemical recycling of carbon dioxide to fuels. *Catal. Today* **2009**, *148*, 191–205.
- (3) Aresta, M.; Dibenedetto, A.; Angelini, A. Catalysis for the valorization of exhaust carbon: from CO₂ to chemicals, materials, and fuels. Technological use of CO₂. *Chem. Rev.* **2014**, *114*, 1709–1742.
- (4) Sudhagar, P.; Roy, N.; Vedarajan, R.; Devadoss, A.; Terashima, C.; Nakata, K.; Fujishima, A. In *Photoelectrochemical solar fuel production: from basic principles to advanced devices*; Giménez, S., Bisquert, J., Eds.; Springer International Publishing: Cham, Switzerland, 2016; pp 105–160.
- (5) Haberreutinger, S. N.; Schmidt-Mende, L.; Stolarsky, J. K. Photocatalytic reduction of CO₂ on TiO₂ and other semiconductors. *Angew. Chem., Int. Ed.* **2013**, *52*, 7372–7408.
- (6) Li, K.; Peng, B.; Peng, T. Recent advances in heterogeneous photocatalytic CO₂ conversion to solar fuels. *ACS Catal.* **2016**, *6*, 7485–7527.
- (7) Yin, W.-J.; Krack, M.; Wen, B.; Ma, S.-Y.; Liu, L.-M. CO₂ capture and conversion on rutile TiO₂ (110) in the water environment: insight by first-principles calculations. *J. Phys. Chem. Lett.* **2015**, *6*, 2538–2545.
- (8) Yin, W.-J.; Wen, B.; Bandaru, S.; Krack, M.; Lau, M.; Liu, L.-M. The effect of excess electron and hole on CO₂ adsorption and activation on rutile (110) surface. *Sci. Rep.* **2016**, *6*, 23298.
- (9) Sorescu, D. C.; Lee, J.; Al-Saidi, W. A.; Jordan, K. D. Co-adsorption properties of CO₂ and H₂O on TiO₂ rutile (110): A dispersion-corrected DFT study. *J. Chem. Phys.* **2012**, *137*, 074704.
- (10) Smith, R. S.; Li, Z.; Chen, L.; Dohnálek, Z.; Kay, B. D. Adsorption, desorption, and displacement kinetics of H₂O and CO₂ on TiO₂(110). *J. Phys. Chem. B* **2014**, *118*, 8054–8061.
- (11) Galhenage, R. P.; Xie, K.; Yan, H.; Seuser, G. S.; Chen, D. A. Understanding the growth, chemical activity, and cluster-support interactions for Pt-Re bimetallic clusters on TiO₂(110). *J. Phys. Chem. C* **2016**, *120*, 10866–10878.
- (12) Dimitrijevic, N. M.; Vijayan, B. K.; Poluektov, O. G.; Rajh, T.; Gray, K. A.; He, H.; Zapol, P. Role of water and carbonates in photocatalytic transformation of CO₂ to CH₄ on titania. *J. Am. Chem. Soc.* **2011**, *133*, 3964–3971.
- (13) Ji, Y.; Luo, Y. Theoretical study on the mechanism of photoreduction of CO₂ to CH₄ on the anatase TiO₂(101) surface. *ACS Catal.* **2016**, *6*, 2018–2025.
- (14) Lin, X.; Yoon, Y.; Petrik, N. G.; Li, Z.; Wang, Z.-T.; Glezakou, V.-A.; Kay, B. D.; Lyubinetsky, I.; Kimmel, G. A.; Rousseau, R.; et al. Structure and dynamics of CO₂ on rutile TiO₂(110)-1×1. *J. Phys. Chem. C* **2012**, *116*, 26322–26334.
- (15) Song, A.; Skibinski, E. S.; DeBenedetti, W. J.; Ortoll-Bloch, A. G.; Hines, M. A. Nanoscale solvation leads to spontaneous formation of a bicarbonate monolayer on rutile (110) under ambient conditions: implications for CO₂ photoreduction. *J. Phys. Chem. C* **2016**, *120*, 9326–9333.
- (16) Li, Y.-F.; Selloni, A. Pathway of photocatalytic oxygen evolution on aqueous TiO₂ anatase and insights into the different activities of anatase and rutile. *ACS Catal.* **2016**, *6*, 4769–4774.
- (17) Sorescu, D. C.; Al-Saidi, W. A.; Jordan, K. D. CO₂ adsorption on TiO₂ (101) anatase: a dispersion-corrected density functional theory study. *J. Chem. Phys.* **2011**, *135*, 124701.
- (18) Gong, X.-Q.; Selloni, A.; Vittadini, A. Density functional theory study of formic acid adsorption on anatase TiO₂(001): geometries, energetics, and effects of coverage, hydration, and reconstruction. *J. Phys. Chem. B* **2006**, *110*, 2804–2811.
- (19) Cheng, T.; Xiao, H.; Goddard, W. A., III Free-energy barriers and reaction mechanisms for the electrochemical reduction of CO on the Cu (100) surface, including multiple layers of explicit solvent at pH 0. *J. Phys. Chem. Lett.* **2015**, *6*, 4767–4773.
- (20) Stuett, F.; Abild-Pedersen, F.; Wu, Q.; Jensen, A. D.; Temel, B.; Grunwaldt, J.-D.; Norskov, J. K. CO hydrogenation to methanol on Cu-Ni catalysts: theory and experiment. *J. Catal.* **2012**, *293*, 51–60.
- (21) Stirling, A.; Pápai, I. H₂CO₃ forms via HCO₃⁻ in water. *J. Phys. Chem. B* **2010**, *114*, 16854–16859.
- (22) Cheng, T.; Xiao, H.; Goddard, W. A., III Reaction Mechanisms for the Electrochemical Reduction of CO₂ to CO and Formate on the Cu (100) Surface at 298 K from Quantum Mechanics Free Energy Calculations with Explicit Water. *J. Am. Chem. Soc.* **2016**, *138*, 13802–13805.
- (23) Cheng, T.; Xiao, H.; Goddard, W. A. Full atomistic reaction mechanism with kinetics for CO reduction on Cu (100) from ab initio molecular dynamics free-energy calculations at 298 K. *Proc. Natl. Acad. Sci. U. S. A.* **2017**, *114*, 1795.
- (24) Valiev, M.; Bylaska, E. J.; Govind, N.; Kowalski, K.; Straatsma, T. P.; van Dam, H. J.; Wang, D.; Nieplocha, J.; Apra, E.; Windus, T. L.; et al. NWChem: a comprehensive and scalable open-source solution for large scale molecular simulations. *Comput. Phys. Commun.* **2010**, *181*, 1477–1489.
- (25) Barducci, A.; Bonomi, M.; Parrinello, M. Metadynamics. *Wiley Interdisciplinary Reviews: Computational Molecular Science* **2011**, *1*, 826–843.
- (26) Laio, A.; Gervasio, F. L. Metadynamics: a method to simulate rare events and reconstruct the free energy in biophysics, chemistry and material science. *Rep. Prog. Phys.* **2008**, *71*, 126601.
- (27) Perdew, J. P.; Burke, K.; Ernzerhof, M. Generalized gradient approximation made simple. *Phys. Rev. Lett.* **1996**, *77*, 3865.
- (28) Troullier, N.; Martins, J. L. Efficient pseudopotentials for plane-wave calculations. *Phys. Rev. B: Condens. Matter Mater. Phys.* **1991**, *43*, 1993.
- (29) Hamann, D. Generalized norm-conserving pseudopotentials. *Phys. Rev. B: Condens. Matter Mater. Phys.* **1989**, *40*, 2980.
- (30) Grimme, S.; Antony, J.; Ehrlich, S.; Krieg, H. A consistent and accurate ab initio parametrization of density functional dispersion correction (DFT-D) for the 94 elements H-Pu. *J. Chem. Phys.* **2010**, *132*, 154104.
- (31) Nosé, S. A molecular dynamics method for simulations in the canonical ensemble. *Mol. Phys.* **1984**, *52*, 255–268.
- (32) Hoover, W. G. Canonical dynamics: equilibrium phase-space distributions. *Phys. Rev. A: At., Mol., Opt. Phys.* **1985**, *31*, 1695.
- (33) Ghoussoub, M.; Yadav, S.; Ghuman, K. K.; Ozin, G. A.; Singh, C. V. Metadynamics-biased ab initio molecular dynamics study of heterogeneous CO₂ reduction via surface frustrated Lewis pairs. *ACS Catal.* **2016**, *6*, 7109–7117.
- (34) Dudarev, S.; Botton, G.; Savrasov, S.; Humphreys, C.; Sutton, A. Electron-energy-loss spectra and the structural stability of nickel oxide: an LSDA+U study. *Phys. Rev. B: Condens. Matter Mater. Phys.* **1998**, *57*, 1505.

- (35) Deskins, N. A.; Rousseau, R.; Dupuis, M. Localized electronic states from surface hydroxyls and polarons in $\text{TiO}_2(110)$. *J. Phys. Chem. C* **2009**, *113*, 14583–14586.
- (36) Setvin, M.; Franchini, C.; Hao, X.; Schmid, M.; Janotti, A.; Kaltak, M.; van de Walle, C. G.; Kresse, G.; Diebold, U. Direct view at excess electrons in TiO_2 rutile and anatase. *Phys. Rev. Lett.* **2014**, *113*, 086402.
- (37) Kumar, N.; Neogi, S.; Kent, P. R.; Bandura, A. V.; Kubicki, J. D.; Wesolowski, D. J.; Cole, D.; Sofo, J. O. Hydrogen bonds and vibrations of water on (110) rutile. *J. Phys. Chem. C* **2009**, *113*, 13732–13740.
- (38) Wendt, S.; Matthiesen, J.; Schaub, R.; Vestergaard, E. K.; Lægsgaard, E.; Besenbacher, F.; Hammer, B. Formation and splitting of paired hydroxyl groups on reduced $\text{TiO}_2(110)$. *Phys. Rev. Lett.* **2006**, *96*, 066107.
- (39) Bikondoa, O.; Pang, C. L.; Ithnin, R.; Muryn, C. A.; Onishi, H.; Thornton, G. Direct visualization of defect-mediated dissociation of water on TiO_2 (110). *Nat. Mater.* **2006**, *5*, 189–192.
- (40) Serrano, G.; Bonanni, B.; Di Giovannantonio, M.; Kosmala, T.; Schmid, M.; Diebold, U.; Di Carlo, A.; Cheng, J.; VandeVondele, J.; Wandelt, K. Molecular ordering at the interface between liquid water and rutile $\text{TiO}_2(110)$. *Adv. Mater. Interfaces* **2015**, *2*, 1500246.
- (41) Sun, C.; Liu, L.-M.; Selloni, A.; Lu, G. Q. M.; Smith, S. C. Titania-water interactions: a review of theoretical studies. *J. Mater. Chem.* **2010**, *20*, 10319–10334.
- (42) Liu, L.-M.; Zhang, C.; Thornton, G.; Michaelides, A. Structure and dynamics of liquid water on rutile $\text{TiO}_2(110)$. *Phys. Rev. B: Condens. Matter Mater. Phys.* **2010**, *82*, 161415.
- (43) Cheng, J.; Sprik, M. Acidity of the aqueous rutile TiO_2 (110) surface from density functional theory based molecular dynamics. *J. Chem. Theory Comput.* **2010**, *6*, 880–889.
- (44) Lee, J.; Sorescu, D. C.; Deng, X.; Jordan, K. D. Water chain formation on $\text{TiO}_2(110)$. *J. Phys. Chem. Lett.* **2013**, *4*, 53–57.
- (45) Brinkley, D.; Dietrich, M.; Engel, T.; Farrall, P.; Gantner, G.; Schafer, A.; Szuchtmacher, A. A modulated molecular beam study of the extent of H_2O dissociation on $\text{TiO}_2(110)$. *Surf. Sci.* **1998**, *395*, 292–306.
- (46) Sommerfeld, T.; Meyer, H.-D.; Cederbaum, L. S. Potential energy surface of the CO_2^- anion. *Phys. Chem. Chem. Phys.* **2004**, *6*, 42–45.
- (47) Liu, L.; Zhao, H.; Andino, J. M.; Li, Y. Photocatalytic CO_2 reduction with H_2O on TiO_2 nanocrystals: Comparison of anatase, rutile, and brookite polymorphs and exploration of surface chemistry. *ACS Catal.* **2012**, *2*, 1817–1828.
- (48) Indrakanti, V. P.; Kubicki, J. D.; Schobert, H. H. Photoinduced activation of CO_2 on Ti-based heterogeneous catalysts: current state, chemical physics-based insights and outlook. *Energy Environ. Sci.* **2009**, *2*, 745–758.
- (49) Indrakanti, V. P.; Kubicki, J. D.; Schobert, H. H. Photoinduced activation of CO_2 on TiO_2 surfaces: Quantum chemical modeling of CO_2 adsorption on oxygen vacancies. *Fuel Process. Technol.* **2011**, *92*, 805–811.
- (50) Kortlever, R.; Shen, J.; Schouten, K. J. P.; Calle-Vallejo, F.; Koper, M. T. Catalysts and reaction pathways for the electrochemical reduction of carbon dioxide. *J. Phys. Chem. Lett.* **2015**, *6*, 4073–4082.
- (51) Liu, L.; Zhao, C.; Li, Y. Spontaneous dissociation of CO_2 to CO on defective surface of Cu (I)/ TiO_{2-x} nanoparticles at room temperature. *J. Phys. Chem. C* **2012**, *116*, 7904–7912.
- (52) Henderson, M. A. Evidence for bicarbonate formation on vacuum annealed $\text{TiO}_2(110)$ resulting from a precursor-mediated interaction between CO_2 and H_2O . *Surf. Sci.* **1998**, *400*, 203–219.
- (53) Pan, D.; Galli, G. The fate of carbon dioxide in water-rich fluids under extreme conditions. *Science Advances* **2016**, *2*, e1601278.
- (54) Wang, X.; Conway, W.; Burns, R.; McCann, N.; Maeder, M. Comprehensive study of the hydration and dehydration reactions of carbon dioxide in aqueous solution. *J. Phys. Chem. A* **2010**, *114*, 1734–1740.
- (55) Stirling, A. HCO_3^- formation from CO_2 at high pH: ab initio molecular dynamics study. *J. Phys. Chem. B* **2011**, *115*, 14683–14687.
- (56) Towns, J.; Cockerill, T.; Dahan, M.; Foster, I.; Gaither, K.; Grimshaw, A.; Hazlewood, V.; Lathrop, S.; Lifka, D.; Peterson, G. D.; et al. XSEDE: accelerating scientific discovery. *Comput. Sci. Eng.* **2014**, *16*, 62–74.